Intracellular Hypertonicity Is Responsible for Water Flux Associated with Na^+/Glucose Cotransport

François M. Charron, Maxime G. Blanchard, and Jean-Yves Lapointe
Groupe d'étude des protéines membranaires (GÉPROM) and Département de Physique, Université de Montréal, Canada

ABSTRACT Detection of a significant transmembrane water flux immediately after cotransporter stimulation is the experimental basis for the controversial hypothesis of secondary active water transport involving a proposed stoichiometry for the human Na^+/glucose cotransporter (SGLT1) of two Na^+, one glucose, and 264 water molecules. Volumetric measurements of *Xenopus laevis* oocytes coexpressing human SGLT1 and aquaporin can be used to detect osmotic gradients with high sensitivity. Adding 2 mM of the substrate α-methyl-glucose (αMG) created mild extracellular hypertonicity and generated a large cotransport current with minimal cell volume changes. After 20, 40, and 60 s of cotransport, the return to sugar-free, isotonic conditions was accompanied by measurable cell swelling averaging 0.051, 0.061, and 0.077 nl/s, respectively. These water fluxes are consistent with internal hypertonicities of 1.5, 1.7, and 2.2 mOsm for these cotransport periods. In the absence of aquaporin, the measured hypertonicites were 4.6, 5.0, and 5.3 mOsm for the same cotransport periods Cotransport-dependent water fluxes, previously assumed to be water cotransport, could be largely explained by hypertonicities of such amplitudes. Using intracellular Na^+ injection and Na^+-selective electrode, the intracellular diffusion coefficient for Na^+ was estimated at $0.29 \pm 0.03 \times 10^{-5}$ cm^2 s^{-1}. Using the effect of intracellular αMG injection on the SGLT1-mediated outward current, the intracellular diffusion coefficient of αMG was estimated at $0.15 \pm 0.01 \times 10^{-5}$ cm^2 s^{-1}. Although these intracellular diffusion coefficients are much lower than in free aqueous solution, a diffusion model for a single solute in an oocyte would require a diffusion coefficient three times lower than estimated to explain the local osmolyte accumulation that was experimentally detected. This suggests that either the diffusion coefficients were overestimated, possibly due to the presence of convection, or the diffusion in cytosol of an oocyte is more complex than depicted by a simple model.

INTRODUCTION

Until the mid-1990s, the dogma that water transport through biological membranes was always passive had never been seriously contested. Water is known to permeate biological membranes via diffusion across the phospholipid bilayer or by using several types of membrane proteins, including the different forms of aquaporin (1–3). In 1996, a study proposed that water can be pumped in a secondary active manner using the rabbit Na^+/glucose cotransporter (SGLT1) in a strictly stoichiometric ratio of two Na^+ ions, one glucose molecule, and ~260 water molecules (4). According to subsequent studies, such a phenomenon was not restricted to SGLT1 and a variety of cotransporters were proposed to carry from 50 to 400 water molecules per turnover (5). We challenged this interesting hypothesis by showing that, in our hands, the swelling induced by the addition of glucose to an oocyte expressing the human SGLT1 is not instantaneous and by calculating that the osmotic gradient detected after several minutes of cotransport was quantitatively sufficient to explain all of the glucose-induced cell swelling (6). In addition, by independently expressing a solute transporter (GLUT1) and a cationic channel (ROMK2), we have shown that the sum of the passive water fluxes associated with glucose and potassium transport matches the cell swelling due to SGLT1 when transporting corresponding amounts of glucose and Na^+ (7). This has led to a certain controversy (7–15), which can be summarized by asking the following question: is it possible to observe water transport (J_w) in the absence of an osmotic gradient ($\Delta\pi$)? Quantitatively, the size of the $\Delta\pi$ expected is J_w/P_f where Pf is the membrane osmotic permeability. In the case of human SGLT1, the cell swelling typically observed after 30 s of maximal Na^+/glucose cotransport corresponds to a $\Delta\pi$ of 4 mOsm (7). According to authors defending the water cotransport hypothesis, all of the cell swelling observed during the first minute of Na^+/glucose cotransport stimulation is due to water cotransport and occurs in the absence of any significant $\Delta\pi$ (9). This hypothesis contends that a significant osmotic gradient caused by transported solute accumulation starts to develop after the first minute and reaches a steady-state condition in 5–10 min. At this time, the osmotic gradient would account for two-thirds of the cell swelling and water cotransport would account for the rest (9). In contrast to this line of thought, we contend that all water transport is passive and that the osmotic gradient starts to develop as soon as cotransport is activated. It is recognized that low intracellular diffusion coefficients for Na^+ and for glucose are required to explain why an osmotic gradient of several mOsm can be generated within the first minute of cotransport.

The first part of the present study establishes a sensitive way of detecting osmotic gradients by using oocytes

Submitted October 27, 2005, and accepted for publication January 8, 2006.

Address reprint requests to Jean-Yves Lapointe, Groupe d'étude des protéines membranaires (GÉPROM), Université de Montréal, C.P. 6128, succ. centre-ville, Montréal, Québec H3C 3J7, Canada. E-mail: jean-yves.lapointe@umontreal.ca.

0006-3495/06/05/3546/09 $2.00

doi: 10.1529/biophysj.105.076745

coexpressing human SGLT1 and aquaporin 1 (AQP1). The second part of the study involves using microinjection of Na^+ and glucose into the center of the oocyte while measuring their peripheral concentrations electrophysiologically to estimate their intracellular diffusion coefficients.

MATERIALS AND METHODS

Oocyte preparation

Xenopus laevis oocytes, stage V–VI, were harvested as recently described by our laboratory (16). SGLT1 mRNA was obtained from transcription of human SGLT1 cDNA (17,18), and the human form of AQP1 was kindly provided by J. M. Verbavatz (CEA/Saclay, Gif-sur-Yvette Cedex, France). We injected 4.6 ng of SGLT1 mRNA (0.1 μg/μl) into oocytes with a Drummond microinjector (Broomall, PA). Oocytes were then kept 5–7 days at 18°C in Barth's solution containing (in mM) 90 NaCl, 3 KCl, 0.82 $MgCl_2$, 0.74 $CaCl_2$, 10 Hepes, and 5% (v/v) horse serum (pH titrated to 7.6 with Tris[hydroxymethyl]aminomethane (Tris)). AQP1 mRNA (4.6 ng) was injected only 1–2 days before the day of the experiment. Expression of AQP1 was tested with a hypotonic shock and oocytes coexpressing AQP1 and SGLT1 were found to have an average water permeability of 4.9×10^{-3} cm s^{-1}, which is more than seven times the permeability of the SGLT1-expressing oocytes used in the present study.

Volumetry

Oocyte volume was measured with a previously described (7) apparatus. Briefly, the cross section of an oocyte was measured with an inverted microscope 5 times/s using a CCD camera and a 3× objective. Software was used to count the number of pixels corresponding to the oocyte cross section. Before analysis, five consecutive data points were averaged to give one measurement per second. Analysis programs for obtaining swelling rates and other measurements were written using Matlab 6.5 (MathWorks, Natick, MA). The hypertonic shock was applied by adding 2 mM (oocytes coexpressing SGLT1 and AQP1) or 5 mM (oocytes expressing only SGLT1) αMG or mannitol to the Barth's solution. Moreover, to rapidly stop SGLT1 after removing αMG when AQP1 was present, 50 μM phlorizin (Pz, the specific inhibitor of SGLT1) was directly added to the Barth's solution. This concentration represents 380 times its K_i value (19).

Two-microelectrode voltage clamp and intracellular Na^+-selective electrodes

The two-microelectrode voltage-clamp method was used as previously described (6) and data were recorded using Clampex 8.1 (Axon Instruments, Union City, CA) software. For simultaneous voltage-clamp and volumetry experiments, the voltage electrode was filled with 1 M KCl and the current electrode was filled with a solution containing (in mM) 70 K-gluconate, 15 KCl, 10 NaCl,and 10 Hepes. During inward current compensation, this type of current electrode produces a reduced injection of Cl^- from the electrode to the cell. The data were taken at a rate of 200 Hz with a membrane voltage of −50 mV. For intracellular Na^+ measurements, the oocytes were not clamped and a single voltage electrode containing 1 M KCl was used. Na^+-selective microelectrodes were made with a Na^+-selective resin (sodium ionophore 1-cocktail A, Fluka, St. Louis, MO), (20). The electrodes were pulled on a Flaming/Brown micropipette puller (Sutter Instrument, Novato, CA) and they have a resistance of 2 MΩ when filled with 1 M KCl. The electrode tip was immersed in a solution of 5% (v/v) dichlorodiphenylsilane in acetone for 20 s. After silanization, the tip was rapidly rinsed with acetone and the electrodes were incubated overnight at 80°C. Before an experiment, the tip was filled with the Na^+-selective resin and the rest of the electrode was filled with a solution of 100 mM NaCl. The signal corresponding to the Na^+ concentration was obtained by subtraction of the oocyte potential from the Na^+-selective electrode potential. The selective electrodes were calibrated with three different concentrations of sodium containing (in mM) 5 NaCl/95 KCl, 10 NaCl/90 KCl, or 100 NaCl/2 KCl with 0.82 $MgCl_2$, 10 Hepes (pH adjusted to 7.6 with Tris). Using the calibration solutions, the selectivity ratio for Na^+ over K^+ was ~100. The Na^+ solution used for intracellular injection contains 100 mM Na-cyclamate and 100 μM EGTA. This solution was used to increase intracellular Na^+ concentration without adding a significant amount of Cl^- or Ca^{2+} to the cytosolic solution. The injection of Na^+ was performed only after the Na^+-selective potential was observed to be stable for at least 1 min. Data were taken every 5 ms.

For measurement of the Na^+ diffusion coefficient in aqueous solution, a distant Ag/AgCl electrode was used to ground the bath solution. An injection pipette filled with (in mM) 750 NaCl and 1899 sucrose (yielding a viscosity of 16 cP) was extended to the bottom of a chamber filled with a solution containing (in mM) 5 NaCl, 95 KCl, and 1840 sucrose (15 cP). The bath has a minimum radius of 1 cm, a height of 1 cm, and was completely filled with the previously described solution. The injected solution was kept slightly more dense than the bath solution to ensure that the injected solution would tend to remain at the bottom of the bath. A Na^+-selective microelectrode was positioned 1 mm distant from the side of the injection pipette to detect the time-dependent increase in the bath Na^+ concentration after the injection of 10 nl of the Na^+ solution. The apparent intracellular Na^+ diffusion coefficient was obtained by measuring the steady-state increase in Na^+ concentration that was reached a few minutes after bath Na^+ injection.

To determine the glucose diffusion coefficient, outward currents through SGLT1 were measured after glucose injection (10 nl of a 500 mM αMG solution) in an oocyte displaying an increased intracellular Na^+ concentration caused by 2 h incubation in a K^+- and Ca^{2+}-free solution containing (in mM) 90 NaCl, 3 NMDG, 0.82 $MgCl_2$, and 10 Hepes at pH 7.6 (21). The outward current was detected at +50 mV in a low Na^+ solution containing (in mM) 10 NaCl, 83 NMDG, 0.82 $MgCl_2$, 0.74 $CaCl_2$, and 10 Hepes at pH 7.6. In this case, the two microelectrodes for voltage clamp were filled with 1 M KCl and a pulse protocol was applied every 30 s, with potential ranging from –75 mV to +50 mV in increments of 25 mV, with the oocytes clamped at –50 mV between series of measurements. The injection of αMG was done right after the tenth pulse at $t = 300$ s. To ensure that the outward currents measured actually arose from SGLT1, some oocytes were perfused with a low Na^+ solution containing Pz, the injection of αMG was performed as before, and Pz was removed at $t = 750$ s.

Volumetric analysis

To obtain instantaneous swelling rates, experimental volume curves were first fitted with an empiric equation that can mimic the time course of the volume measurement for a given experimental period. The linear portion of the volume versus time curves during an osmotic shock with mannitol ($\Delta\pi$, in mol/cm^3) was simply fitted with a straight line for oocytes expressing SGLT1 to obtain P_f, the water permeability, from the following equation:

$$\frac{dV}{dt} = -\bar{v}_w S P_f \Delta\pi, \quad (1)$$

where $\bar{v}_w$ is the specific volume of water (18 cm^3 mol^{-1}) and S is a standard oocyte surface area (0.4 cm^2).

In the case of oocytes coexpressing SGLT1 and AQP1, the volume vs time curves during a purely osmotic shock was not linear and the initial shrinking rate was obtained by fitting the curve with the following exponential equation.

$$\frac{dV}{dt} = m_0 + dm(1 - \exp(-t/\tau)). \quad (2)$$

This represents a cell swelling rate that goes from m_o to $m_o + dm$ with a characteristic time constant of τ. For a given experimental period, the values

for the three parameters that minimized the χ-square were obtained using Origin 6.1 software (OriginLab Corporation, Northampton, MA). The following equation was used to fit the cell volume changes after glucose withdrawal from oocytes expressing SGLT1:

$$\frac{dV}{dt} = m_0 + \frac{dm_a}{1 + e^{-k_a(t-t_a)}} + dm_b(1 - \exp(-t/\tau_b)). \quad (3)$$

This represents an initial cell swelling rate described by a Boltzmann equation that goes from m_o to $m_o + dm_a$ at $t \sim t_a$, with a rate constant of k_a. The swelling rate (dV/dt) is then allowed to go from $m_o + dm_a$ to a final value of $m_o + dm_a + dm_b$, with an exponential time course characterized by a time constant τ_b. For a given experimental period, the seven parameters that minimize the χ-square were found to provide a smooth curve that closely followed the experimental points. In the case of oocytes expressing both SGLT1 and AQP1, Eq 3 could not be used because volume changes were rapid during the first few seconds after glucose withdrawal and much slower afterward, generating a sharp bend in the volume versus time curve (Fig. 1 *B*). In this case, the slope of the volume versus time curve could be satisfactorily fitted with a double Boltzmann equation as follows:

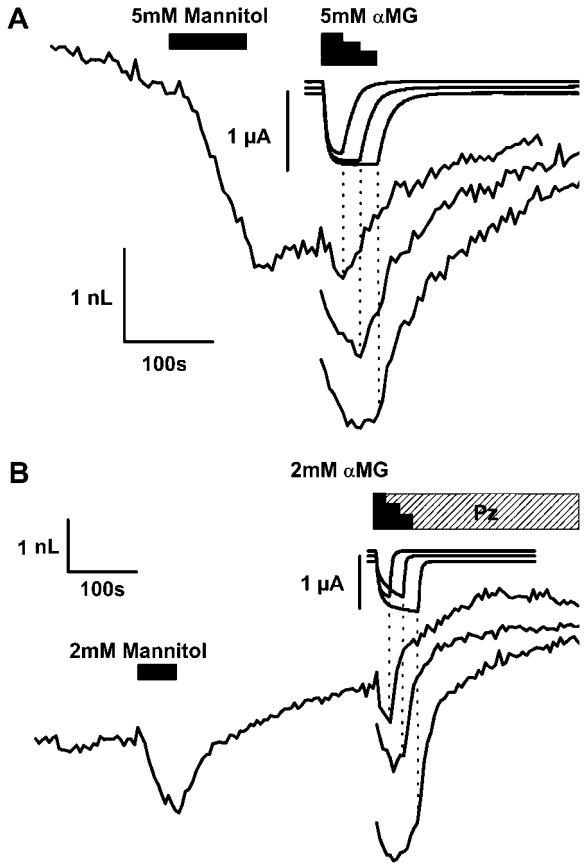

FIGURE 1 Oocyte volume measurements during the hypertonic application of mannitol or αMG. (*A*) Volume of an oocyte expressing SGLT1 that was exposed to 5 mM mannitol and then to 5 mM αMG for three different time periods (20, 40, and 60 s), the recordings from which have been superimposed (both current and volume measurements). The currents at –50 mV and the volume measurements are aligned to the moment of αMG addition. (*B*) The same type of experiment as in panel *A*, but with an oocyte coexpressing SGLT1 and AQP1. Because of the larger water permeability of this type of oocyte, 2 mM mannitol or αMG were used and the cotransport was stopped after 20, 40, or 60 s by simultaneous addition of Pz (50 μM) and removal of αMG.

$$\frac{dV}{dt} = \frac{dm_a}{1 + e^{-k_a(t-t_a)}} + \frac{dm_b}{1 + e^{-k_b(t-t_b)}}. \quad (4)$$

This equation describes a swelling rate that goes from 0 to $dm_a + dm_b$, with two steps occurring at distinct time points (t_a and t_b) and with distinct rate constants (k_a and k_b). Adjustment of these six arbitrary parameters was found sufficient to provide a satisfactory fit to the experimental curves.

Diffusion model

A virtual oocyte of a given volume was first divided into the required number of concentric shells, each representing a constant volume of 40 nl. A typical 1-μl oocyte would then be divided into 25 shells with thicknesses ranging from 134 μm in the center to 8.5 μm in the periphery. A fraction V_A of the volume is considered to be freely accessible to water and osmolytes. A single type of osmolyte is considered and its concentration in each shell (C_i) is set to 200 mOsm at $t = 0$. For each time increment (dt) of 0.02 s, osmolyte uptake into the most external shell (C_1) is calculated from the amount of charge carried by the measured cotransport current (I) as follows:

$$dOsm = \frac{I \times dt}{F} \times opc, \quad (5)$$

where $dOsm$ is the number of moles of solute accumulated during a time increment dt, F is the Faraday constant, and opc is the net number of osmolytes per transported charge that are entering the oocyte through the plasma membrane or through the current-injecting electrode. When measuring a purely ionic transport generated through a K channel (ROMK2), the type of current-injecting electrode used generated 0.65 osmolyte for each K^+ ion entering the oocyte. This indicates that in the case of SGLT1, each Na^+ entering the oocyte is accompanied by 0.65 osmolyte and 0.5 glucose molecule, which yields an opc of 1.15. This was used to calculate a new C_1 for $t = 0+ dt$. Then diffusion was allowed to occur between consecutive shells using Fick's first law:

$$J_{i,i+1} = D\frac{(C_i - C_{i+1})}{(r_i - r_{i+1})}, \quad (6)$$

where $J_{i,i+1}$ is the flux of osmolyte from shell i to shell $i + 1$, D is the osmolyte diffusion coefficient, and r_i is the radius of shell i. These fluxes are used to calculate the net uptake into each shell and a new C_i. Finally, the new C_1 is used to calculate water transport across the plasma membrane using Eq. 1. The program was written with Matlab 6.5 and was used to reproduce cell volume during an experiment where hypertonic αMG was used to stimulate a cotransport current. As the water permeability was measured for each oocyte, only two parameters needed to be adjusted, the intracellular diffusion coefficient (D) and the accessible volume fraction V_A, which was found to vary within very tight limits ($0.45 < V_A < 0.65$).

The same program was used to model a wide variety of diffusion processes exhibiting spherical symmetry, yielding the Na^+ diffusion coefficient both in bulk aqueous solution and in an oocyte where 10 nl Na cyclamate solution (100 mM) was injected into the center shell of the oocyte and the Na^+ concentration was measured at the periphery with a Na^+-selective microelectrode. In this latter case, the cotransport current was set at 0 throughout the modeling and no water transport was calculated across the plasma membrane. The same approach was used to model αMG diffusion (10 nl central injection of a 500 mM αMG solution) from the point of injection to the plasma membrane where it was detected as a phlorizin-sensitive outward current periodically measured at +50 mV. The values of D and V_A were adjusted manually until a satisfactory fit was obtained for the time course of the oocyte volume, the peripheral Na^+ concentration, or the appearance of a glucose-dependent outward current.

RESULTS

Detection of transport-dependent osmotic gradients

To facilitate the detection of transport-dependent intracellular osmolyte accumulation and to minimize the dilution caused by the concomitant cell swelling, we sought to reproduce the experiment published by Meinild et al. (22). In that experiment, 10 mM αMG was added hypertonically to the bathing solution to simultaneously produce a hypertonic shock and a large cotransport current through the rabbit SGLT1 protein. In our hands, the water efflux caused by the hypertonic shock was much stronger than the water influx caused by the activation of the human Na^+/glucose cotransporter. We thus compromised by using the protocol illustrated in Fig. 1 *A*, where an oocyte expressing SGLT1 was first exposed to a hypertonic solution containing 5 mM mannitol before being successively exposed to 5 mM αMG for 20, 40, and 60 s, with stabilization periods in isotonic Barth's solution between each cotransport period. The large effect produced by the hypertonic shock with mannitol allows calculation of the oocyte P_f (see Eq. 1), which averaged $6.5 \pm 0.8 \times 10^{-4}$ cm s^{-1}, in good agreement with previous measurements by this laboratory and others for oocytes expressing human SGLT1 (6,10,23). In contrast to the observations published by Meinild et al., addition of 5 mM αMG always produced an initial cell shrinkage (due to the hypertonic shock), which was progressively reversed after 10–15 s of cotransport. Interestingly, after each of the cotransport periods, when the oocyte was returned to isotonic Barth's solution, a large cell swelling was consistently observed. This behavior was also observed in the work of Meinild et al. (22) but was not analyzed. Upon αMG removal, the cotransporter no longer cotransports Na^+ and glucose (and water if the water cotransport hypothesis is true) into the cell and, as the extracellular solution is isotonic, the large cell swelling observed has to be due to the presence of an intracellular hypertonicity that has developed during the cotransport period.

The sensitivity of this experiment can be greatly improved by increasing the oocyte P_f through coexpression of SGLT1 with AQP1 (24). This is shown in Fig. 1 *B*, where the hypertonic shock caused by addition of 2 mM mannitol generates a rapid cell shrinkage consistent with an increased P_f (average $P_f = 49 \pm 5 \times 10^{-4}$ cm s^{-1}, n= 10, i.e., more than seven times the P_f of SGLT1-expressing oocytes). The fact that, under these circumstances, the passive phlorizin-sensitive water permeability of SGLT1 represents <10% of the total *Pf* allowed us to terminate the transport period more abruptly by adding 50 μM Pz to the isotonic Barth's solution instead of simply removing αMG. Strongly supporting experiments performed with SGLT1, oocytes coexpressing SGLT1, and AQP1 display very fast cell swelling upon return of the oocyte to an isotonic, phorizin-containing solution (Fig. 1 *B*).

A quantitative analysis of the type of experiments shown in Fig. 1, *A* and *B*, can be performed after fitting the volume curves with an appropriate equation, as explained in Materials and Methods. An example of a fitting result is presented in Fig. 2 for an oocyte expressing both SGLT1 and AQP1. First, it is obvious that, due to the large P_f of the expressed AQP1, the shrinking rate produced by the addition of 2 mOsm mannitol does not remain constant with time. The cell shrinkage was fitted with an exponential function from which the initial slope was used to accurately calculate the oocyte P_f. Eq. 4 was used to precisely fit each phase of the volume changes after the cotransport period was finished. Knowing the P_f and the time derivative of the volume curve (from Eq. 4), it is possible to calculate the amplitude of the local osmotic gradient throughout this period. The result of this type of analysis is shown in Fig. 3 *A* for a series of 10 oocytes expressing SGLT1. The osmotic gradients measured 5 s after the termination of the cotransport periods are 4.6 ± 0.9, 5.0 ± 0.7, and 5.3 ± 0.5 mOsm for 20 s, 40 s, and 60 s cotransport periods, respectively (mean $\pm$ SEM, $n = 10$ oocytes obtained from three different donors). In the case of oocytes coexpressing SGLT1 and AQP1, Fig. 3 *B* shows that the swelling rate experimentally observed 5 s after the cotransport period has been terminated by addition of Pz indicates that osmotic gradients of 1.5 ± 0.2, 1.7 ± 0.3, and 2.2 ± 0.2 mOsm were present after transport periods of 20 s, 40 s, and 60 s, respectively (mean of 12 oocytes obtained from three different donors). It should be noted that the osmotic gradients calculated after different cotransport periods are estimated while cotransport is either blocked with Pz or inactivated by the absence of glucose. In consequence, the cell swelling used to calculate these gradients cannot depend on the capacity of SGLT1 to perform secondary active water transport.

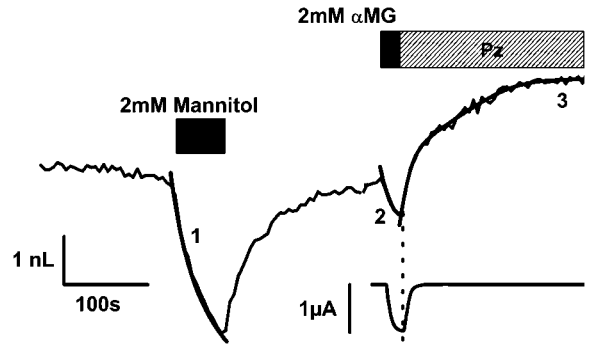

FIGURE 2 Example of curve-fitting results for a typical oocyte coexpressing SGLT1 and AQP1. The oocyte was exposed to a brief hypertonic shock (2 mM mannitol); later, the cotransport current was stimulated for 20 s by the hypertonic addition of 2 mM αMG. The smooth line labeled 1 is obtained from fitting a simple exponential function to the volume reduction caused by the hypertonic shock. The smooth line labeled 2 is drawn from Eq. 2 and mimics the cell shrinkage due to a combined hypertonic shock and stimulation of Na^+/glucose cotransport. Finally, the curve labeled 3 represents a double Boltzmann equation (obtained using Eq. 4) fitting the rapid cell swelling that follows the cotransport inhibition and the return to an isotonic solution.

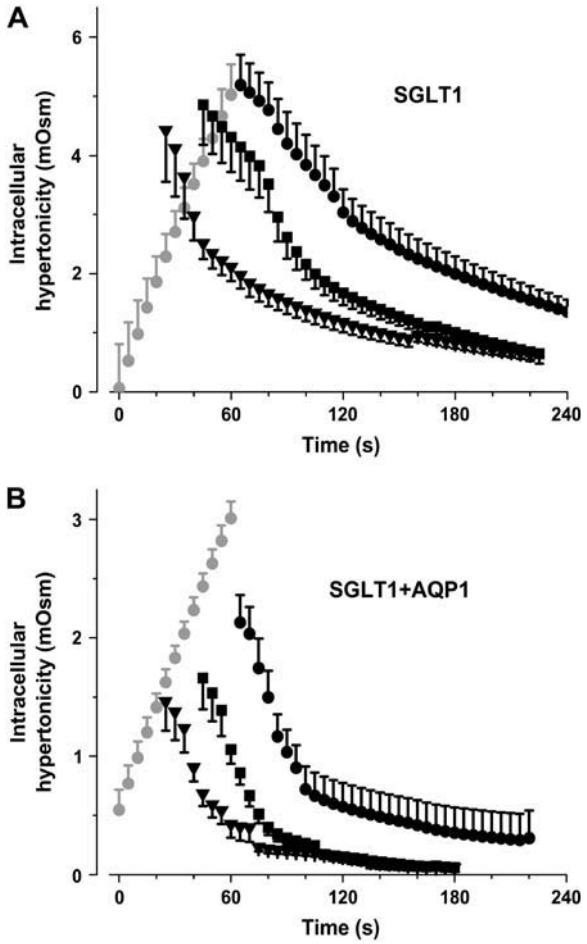

FIGURE 3 Progression of changes in intracellular hypertonicity after cotransport periods of 20 (*triangles*), 40 (*squares*), and 60 s (*circles*). (*A*) Changes in intracellular tonicities as averaged from 10 different SGLT1-expressing oocytes. Data shown in gray represent the calculated changes in intracellular hypertonicities during the cotransport periods of 60 s with the assumption that all water transport is passive. Data shown in black represent the changes in hypertonicity after cotransport has been halted by removal of substrate. (*B*) Average changes in intracellular hypertonicities for 12 oocytes expressing SGLT1 and AQP1. Data shown in black represent the changes in hypertonicity after cotransport has been halted by simultaneous removal of substrate and addition of inhibitor.

If it is assumed that water transport is always passive, the build-up of the osmotic gradients during cotransport stimulation can be calculated from the slope of the volume versus time curve. If the assumption is correct, the predicted rise in intracellular osmolarity should lead to the osmolarity measured at the beginning of the period where cotransport is inactivated. Each volume versus time trace during cotransport activation was fitted and the dV/dt calculated with Eq. 2 at 5-s intervals. Using the P_f obtained for each experiment, the build-up of the osmolarity gradient was estimated, and the results are shown in Fig. 3, *A* and *B* (*gray solid circles*) for the experiments performed with oocytes expressing SGLT1 or SGLT1 + AQP1 and for a cotransport period of 60 s. For oocytes expressing only SGLT1, the build-up of intracellular osmolarity matches the osmolarity gradient detected in the post-cotransport period. This indicates that the intracellular osmolarity detected during the first few seconds of the post-cotransport period is exactly the value required to explain all of the volume change observed during the cotransport period in the presence of a 5-mOsm hypertonic αMG solution. In the case of oocytes coexpressing SGLT1 and AQP1, the gradients detected in the post-cotransport period correspond to 67% and 70% of the intracellular osmolarity gradient calculated after 40 s and 60 s, respectively. This suggests that at least 67% and 70% of the cell-volume changes associated with cotransport activation are passive after 40 s or 60 s of cotransport. This contrasts with the prediction of the water cotransport hypothesis, which purports that 0% of the water transport would be passive during the first minute of cotransport.

Modeling osmolyte accumulation

It is now evident that a significant osmotic gradient can be experimentally detected across the plasma membrane at the end of cotransport periods as short as 20 s. We have used the oocyte model described in Materials and Methods to estimate the size of the intracellular diffusion coefficient that would be required to accumulate these quantities of transported osmolytes near the plasma membrane. This model was applied to oocytes expressing SGLT1 alone because the high water permeability of AQP1 generates larger water fluxes that contribute to dilute the cotransport-dependent osmotic gradient and, consequently, tend to reduce the influence of slow intracellular diffusion. An example of the application of this model is shown in Fig. 4. The model was fitted to the data for each oocyte using the P_f measured for

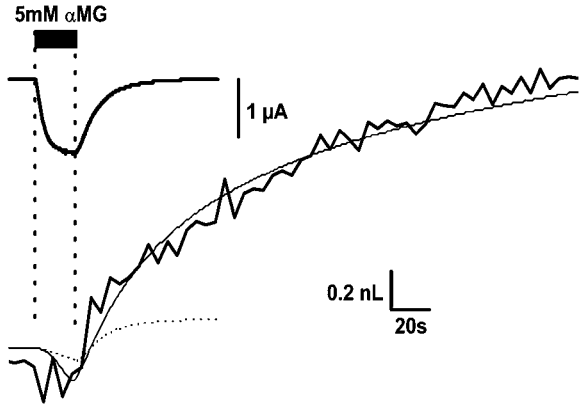

FIGURE 4 Modeling cell swelling during and after hypertonic application of 5 mM αMG for 20 s to an oocyte expressing SGLT1. A simulation of the passive water transport is presented with diffusion coefficients set at 0.030×10^{-5} cm^2 s^{-1} (*upper smooth curve*). The accessible volume fraction was set at 0.61 and the number of osmolytes per transported charge was 1.37. A simulation of active water cotransport was done (*lower smooth curve*) using a stoichiometry of 264 water molecules per turnover and the water permeability measured for this oocyte (9×10^{-4} cm s^{-1}).

that oocyte, and the average value for the number of osmolytes per charge (*opc*) was 1.37 ± 0.54. The accessible volume was fixed at 61%, in agreement with the values obtained by measuring the steady-state increase in intracellular Na^+ concentration after Na cyclamate injection (see below). The only parameter that required adjustment was the diffusion coefficient, which averaged 0.05 ± 0.02 × 10^{-5} cm^2 s^{-1} ($n = 10$ experiments with 20-s cotransport periods). Modeling the experiments with cotransport periods of 40 s and 60 s yielded average diffusion coefficients of 0.05 ± 0.01 × 10^{-5} cm^2 s^{-1} and 0.06 ± 0.01 × 10^{-5} cm^2 s^{-1}, respectively ($n = 10$ experiments). These values are ~10 times smaller than the diffusion coefficient for glucose in free aqueous solution (25). This result can be compared with the prediction based on the water cotransport hypothesis. The lower smooth curve in Fig. 4 is obtained using the measured cotransport current, a stoichiometry of 264 water molecules per glucose molecule transported and the measured P_f for this oocyte. The time course of the change in αMG concentration was estimated from the time course of the cotransport current using an αMG affinity of 0.77 mM. It can be seen that during the 20-s cotransport period, the putative water cotransport is largely neutralized by the effect of external hypertonicity (+5 mOsm). After replacement of the hypertonic αMG solution by the isotonic saline solution, a minimal cell swelling is observed for a short period of ~20 s. This is in clear contrast to the prolonged cell swelling observed experimentally in the present study (Figs. 1, 2, and 4) and in the previous studies of Meinild et al. (22).

Measurements of diffusion coefficient

The Na^+ intracellular diffusion coefficient was measured as described in Materials and Methods, using a central 10-nl intracellular injection of a 100-mM Na-cyclamate solution and a Na^+-selective electrode positioned at the periphery of the oocyte cytoplasm. An example of Na^+ concentration ($[Na^+]_i$) measurement is shown in Fig. 5 *A* (*upper jagged line*). In 17 oocytes obtained from three different donors, the average intracellular $[Na^+]_i$ was 8.5 ± 0.5 mM. Fig. 5 *A* presents the average of 12 measurements of the change in $[Na^+]_i$ during the injection of Na-cyclamate. The transport model was used to fit the time course of the change in $[Na^+]_i$ for each experiment of the type shown in Fig. 5 *A*. The total increase in $[Na^+]_i$ is consistent with a freely accessible volume of 61 ± 5% and the average intracellular diffusion coefficient for Na^+ was estimated at 0.29 ± 0.03 × 10^{-5} cm^2 s^{-1}. In contrast, when 10 nl of water are injected into the center of the oocyte, the measured $[Na^+]_i$ was observed to decrease by 0.4 mM which is consistent with the starting $[Na^+]_i$, the volume injected, and an accessible oocyte volume of 61% (Fig. 5 *A*, *lower jagged line*).

The αMG diffusion coefficient was also measured in the oocyte cytosol using a 10-nl injection of 500 mM αMG at the center of an oocyte expressing SGLT1. When the injected αMG reaches the membrane, the outward current will increase and, given the low intracellular sugar affinity (26,27), it should change in proportion to the local αMG concentration in the vicinity of the membrane (Fig. 5 *B*, *square symbols*). The specificity of the measurements can be demonstrated by the fact that the change in the outward current measured is fully sensitive to the presence of external Pz. For this analysis, an accessible volume of 61% was used and the smooth line in Fig. 5 *B* was obtained with the diffusion model by adjusting the αMG diffusion coefficient to best fit the experimental data. On average, for 11 experiments with oocytes from three different donors, the intracellular diffusion coefficient for αMG was 0.15 ± 0.01 × 10^{-5} cm^2 s^{-1}.

Finally, we checked that measurement of Na^+ diffusion coefficient was possible in free solution by using microinjectors, Na^+-selective microelectrodes, and diffusion distances of the order of 1 mm. In particular, we wanted to check for the presence of convection effects as the 10-nl aliquots were injected. Convection effects were readily observed if Na^+ diffusion was attempted in simple saline solutions. These effects were characterized by rapid and unstable Na^+ concentration changes. It was found that the solution viscosity had to be increased to at least 15 cP (adding 1840 mM sucrose) to make the convection effect much smaller. Such an experiment is shown in Fig. 5 *C*, where Na^+ concentration is measured with a Na^+-selective microelectrode located 1.0 mm away from an injection pipette, which was used to release 10 nL of a 750-mM NaCl solution. Fig. 5 *C* shows an average of four experiments of this type. It can be seen that ~350 s are required to obtain a steady-state rate of Na^+ concentration increase. Using the diffusion model, the diffusion coefficients required to reach the observed rate of increase in the Na^+ concentration average 0.09 ± 0.04 × 10^{-5} cm^2 s^{-1} ($n = 4$). If the experimental measurement is compared with the diffusion model prediction, it can be seen that the measured Na^+ concentration rises much faster than expected (Fig. 5 *C*) during the first 300 s after NaCl injection. This is believed to be due to some convective effect that causes a small quantity of Na^+ to appear faster than expected in the vicinity of the Na^+ electrode. After 300 s, this convective effect has largely ended and the local Na^+ concentration changes at a rate that is consistent with the diffusion coefficient reported above. If the viscosity of water is 0.9548 cP (25), the Na^+ diffusion coefficient in 15 cP sucrose solution is calculated to be 0.084 × 10^{-5} cm^2 s^{-1}. This is <6% smaller than the experimentally estimated coefficient.

DISCUSSION

The aim of the present study was twofold: 1), to measure the size of the osmotic gradient generated within the first minute of Na^+/glucose cotransport; and 2), to explain the generation of this osmotic gradient by slow intracellular diffusion of Na^+ and glucose. We will discuss these points separately.

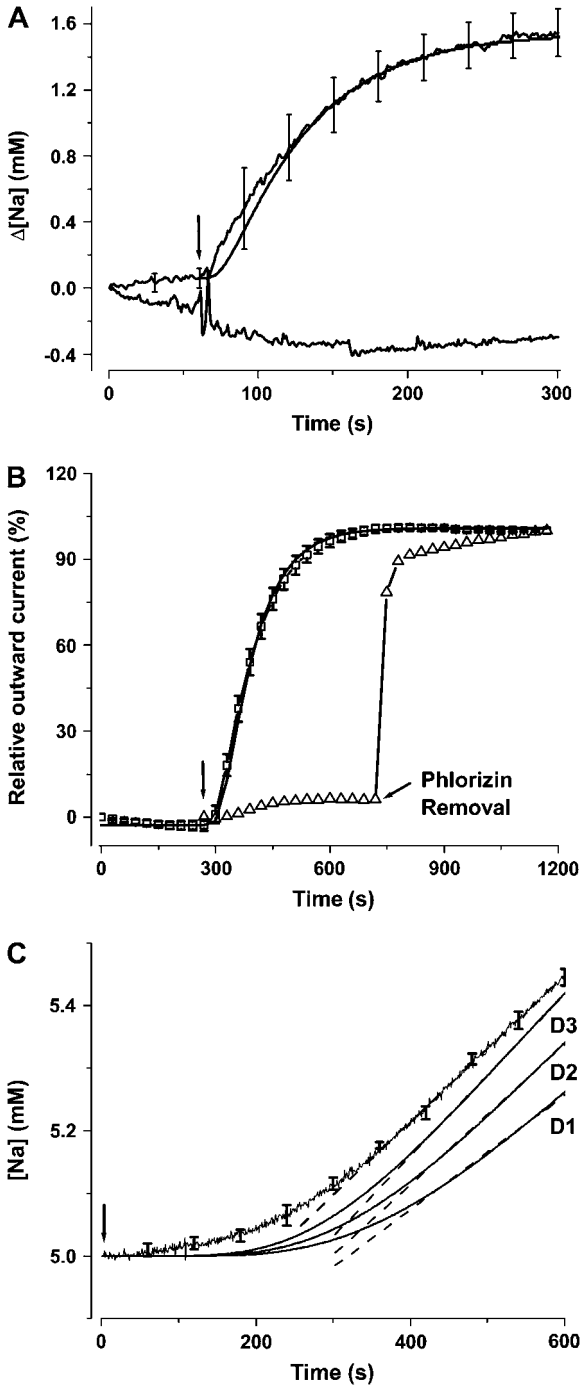

FIGURE 5 Experimental determination of diffusion coefficients for Na^+ and for αMG. Injections were done at points indicated by the arrows in all cases. (*A*) Average of 12 measurements of Na^+ concentration in the periphery of an oocyte after the central injection of 10 nl of 100 mM sodium cyclamate at $t = 60$ s. As the resting $[Na^+]$ varies between oocytes, changes from the resting $[Na^+]$ are shown for reasons of clarity. The rise in Na^+ concentration was fitted with the diffusion model and gave an average diffusion coefficient of 0.29×10^{-5} cm^2 s^{-1} (*solid line*). The bottom jagged trace represents the Na^+ concentration after a central injection of 10 nl water (mean of three oocytes). (*B*) Determination of the diffusion coefficient for αMG. αMG was injected (10 nl of 500-mM αMG solution) in the center of oocytes expressing SGLT1. The αMG concentration in the plasma membrane vicinity was detected by measuring the electrogenic efflux of Na^+ and αMG through SGLT1 using brief voltage clamps at +50 mV every 30 s (*open squares*). The αMG concentration, assumed to be proportional to the outward current, was fitted with the diffusion model and gave an average diffusion coefficient of 0.15×10^{-5} cm^2 s^{-1} (*solid line passing through open squares*). An experiment employing Pz was used as a control to show that the αMG signal was specific to SGLT1; Pz was removed after 12 min (*line with triangles*). (*C*) Determination of the diffusion coefficient for Na^+ in a viscous sucrose solution. A 10-nl amount of 750 mM sodium chloride with a viscosity of 16 cP was injected into the center of a bath containing a saline solution of 15 cP viscosity and a Na^+-selective electrode was used to measure the sodium concentration at 1 mm from the injection site (*jagged line*). The steady-state rise in Na^+ concentration (average of four experiments; error bars represent SE measured at every minute) was fitted with a linear equation (*dashed line*) to be comparable to the predictions of the diffusion model. Three different diffusion coefficients were used: 0.08 (D1), 0.09 (D2), and 0.1×10^{-5} cm^2 s^{-1} (D3). Each curve was used as a calibration curve whose linear part was fit with a linear regression (*dashed lines*). The average diffusion coefficient found from four similar experiments was 0.09×10^{-5} cm^2 s^{-1}.

Presence of a transport-dependent osmotic gradient

Increasing the water permeability of an oocyte with AQP1 enables the detection of osmotic gradients with improved sensitivity. The most direct evidence for the presence of an osmotic gradient after cotransport periods as short as 20 s is the observation of a vigorous cell swelling that occurs as the cotransport period is terminated by the addition of a Pz-containing isotonic extracellular solution (Fig. 1 *B*). Even in the absence of AQP1, the cell swelling can be observed once cotransport is terminated (Fig. 1 *A*). However, the cotransporter cannot be stopped instantaneously at the end of the cotransport period and averages of 6 and 20 s are required for reducing the cotransport current to <20% of its initial value by either adding Pz or removing glucose, respectively. Careful analysis of Fig. 3, *A* and *B*, shows that a large fraction of the osmotic gradient (and its associated cell swelling) is still present at a time when 80% of the cotransport current has disappeared.

If one compares Fig. 1 *A* of this study with Fig. 2 of Meinild et al. (22) (both using human SGLT1), one can notice a few differences between the reported observations. In the case of Meinild et al., activation of the cotransporter by 10 mM αMG can apparently generate an immediate water flux that compensates the concomitant 10-mOsm hypertonic shock. In our case, the 5-mOsm hypertonic shock is always more potent than the cotransport-mediated water flux and an initial cell shrinkage was systematically observed in the first 20–40 s of the cotransport period. This is not due to the difference in αMG concentrations since, with an affinity of 0.77 mM, SGLT1 must have been maximally stimulated in both cases. Further analysis shows that the oocyte used by Meinild et al. was generating an unusually high cotransport current of 2.4 μA (estimated from the integrated current shown in their Fig. 2 *B*) and an unusually low P_f for an oocyte putatively expressing SGLT1 at an extremely high

density. We found only one additional publication, also by Meinild et al. (28), presenting this type of experiment. In Fig. 5 of their article, the effect of a hypertonic application of 10 mM citrate for the Na-dicarboxylate cotransporter is presented. In this case, and in agreement with our observations, an initial shrinking was observed before cotransport-dependent cell swelling starts to compensate. In all cases (this study and those of Meinild et al. (22,28)), returning to isoosmotic and substrate-free solution is associated with a very significant cell swelling. The rate of cell swelling after cotransport period of 60 s was consistent with intracellular hypertonicities of 13 mOsm for the hSGLT1-expressing oocyte (22) and 6 mOsm for NaDC1 cotransporter (28).

Fig. 3, *A* and *B*, clearly shows that the osmotic gradient detected in the post-cotransport period is fully consistent with the rate of cell swelling observed during the first minute of cotransport if all water flux is assumed to be passive. In other words, the intracellular hypertonicity required to account for the observed swelling rate after 60 s of cotransport matches the true hypertonicities experimentally measured immediately after inhibiting the cotransporter. In contrast, according to the water cotransport hypothesis, all water transport in the first minute of cotransport is stoichiometrically coupled to the Na^+/sugar cotransport (9) and the hypertonicity measured at the end of this period is consequently predicted to be negligible. In the case of oocytes expressing AQP1 + SGLT1, the hypertonicity measured immediately after inhibiting cotransport with phlorizin is only 70% of the calculated hypertonicity at the end of the cotransport period (Fig. 3 *B*). A part of this difference can be explained by the fact that the effect of phlorizin on P_f (expected to cause an underestimation of $\Delta\pi$ by 7%) (see Duquette et al. (6) and Loo et al. (23)) has not been taken into account. In summary, an osmotic gradient can be experimentally detected well within the first minute of cotransport and the size of this osmotic gradient is fully consistent with the size required to explain cotransport-dependent cell swelling as a completely passive mechanism.

Low intracellular diffusion coefficients

In our effort to measure the diffusion of Na^+ in water, a convection current was obvious for viscosities ranging from 1 cP to 6 cP. Even at 15 cP, the initial rise in Na^+ concentration measured between 50 and 300 s is still somewhat faster than expected (Fig. 5 *C*). This is why we choose to rely on the steady-state $d[Na^+]/dt$ that could be observed between 300 and 600 s. Theoretically, after the injection of a concentrated NaCl solution, the value of $d[Na^+]/dt$ is expected to go from 0 to a maximal value and return to 0 as a function of time. Using Fick's Second Law, it can be shown that the maximal value of $d[Na^+]/dt$ is strictly proportional to the Na diffusion coefficient. Using this type of analysis and comparing the slope of the linear part of the $[Na^+]$ versus time curve to the slope predicted by our diffusion model, we found that the diffusion coefficient for Na^+ averaged $0.09 \pm 0.04 \times 10^{-5}$ cm^2 s^{-1}. This result follows the Stoke-Einstein equation, which dictates that the diffusion coefficient of a solute is inversely proportional to the viscosity of the solution. As noted in the Results section, our measurement is within 6% of this theoretical prediction. Interestingly, the viscosity of an oocyte cytosol is expected to be between 10 and 30 cP (29). This supports the applicability of our protocol for measuring intracellular diffusion coefficients using intracellular injection and diffusion distances on the order of 1 mm. It also suggests that convective flow is likely to be more important in the initial phase of the Na^+ concentration rise than in the later phase. This is probably what explains the difference between the experimental observations and the predictions from a strictly diffusive model for the first 50 s after intracellular injection (Fig. 5 *A*). Because of the possibility that convective flow may play a role in the early detection of peripheral Na^+ or glucose concentrations, it was decided to adjust the theoretical prediction to best fit changes during the final half of the measurements involving Na^+ or glucose injection.

Slow intracellular diffusion and osmolyte accumulation

For both Na^+ and glucose, the intracellular diffusion coefficients were found to be four to five times smaller than the values reported in free aqueous solutions. In contrast, when the diffusion model was used to reproduce the cell swelling that follows a cotransport period of 20 s (Fig. 4), the required diffusion coefficient for an idealized, transported solute (representing both glucose and Na^+) was $0.05 \pm 0.02 \times 10^{-5}$ cm^2 s^{-1}, which is three times smaller than the slowest diffusion coefficient measured (i.e., 0.15×10^{-5} cm^2 s^{-1} for glucose). This indicates either that our experimental determination of intracellular diffusion coefficients has led to an overestimation of the true values or that the model used to account for intracellular diffusion in an oocyte does not reflect the complexity of the problem. Aside from the inherent differences in the behavior of neutral and charged solutes, as has already been discussed in a previous publication (7), it is important to mention that the diffusion model assumes that the oocyte cytosol is homogeneous. For example, it was not taken into account that the position of the nucleus in the animal pole would affect (speed up or slow down) diffusion on that side of the oocyte. Also, it was not taken into account that the possible damage produced around the injection pipette could represent a ''fast track'' for the diffusion of the injected solute.

CONCLUSION

Osmotic gradients are clearly present within the first minute of cotransport and they have been experimentally detected in a manner that is independent of the properties of SGLT1.

The osmotic gradients are of the size required to explain a dominant portion (from 70% to 100%) of the cotransport-dependent cell swelling. The intracellular diffusion coefficients estimated for Na^+ and glucose are about five times smaller than in free solution but are still not low enough to explain the observed osmolyte accumulation using a simple diffusion model of an oocyte. This can either reflect some overestimation in the actual intracellular diffusion coefficients or a failure of our simple diffusion model to account for the complexity of diffusion in an oocyte.

This work was supported by CIHR (MOP-10580) and F.C. received a scholarship from ''le Fonds Québecois de la recherche sur la nature et les technologies'' (FQRNT).

REFERENCES

1. Agre, P., G. M. Preston, B. L. Smith, J. S. Jung, S. Raina, C. Moon, W. B. Guggino, and S. Nielsen. 1993. Aquaporin CHIP: the archetypal molecular water channel. *Am. J. Physiol.* 265:F463–F476.
2. Hernandez, J. A., and J. Fischbarg. 1992. Kinetic analysis of water transport through a single-file pore. *J. Gen. Physiol.* 99:645–662.
3. Hu, P., S. Meyers, F. X. Liang, F. M. Deng, B. Kachar, M. L. Zeidel, and T. T. Sun. 2002. Role of membrane proteins in permeability barrier function: uroplakin ablation elevates urothelial permeability. *Am. J. Physiol. Renal Physiol.* 283:F1200–F1207.
4. Loo, D. D., T. Zeuthen, G. Chandy, and E. M. Wright. 1996. Cotransport of water by the Na+/glucose cotransporter. *Proc. Natl. Acad. Sci. USA.* 93:13367–13370.
5. MacAulay, N., S. Hamann, and T. Zeuthen. 2004. Water transport in the brain: role of cotransporters. *Neuroscience.* 129:1031–1044.
6. Duquette, P. P., P. Bissonnette, and J. Y. Lapointe. 2001. Local osmotic gradients drive the water flux associated with Na(+)/glucose cotransport. *Proc. Natl. Acad. Sci. USA.* 98:3796–3801.
7. Gagnon, M. P., P. Bissonnette, L. M. Deslandes, B. Wallendorff, and J. Y. Lapointe. 2004. Glucose accumulation can account for the initial water flux triggered by Na+/glucose cotransport. *Biophys. J.* 86:125–133.
8. Lapointe, J. Y., M. P. Gagnon, D. G. Gagnon, and P. Bissonnette. 2002. Controversy regarding the secondary active water transport hypothesis. *Biochem. Cell Biol.* 80:525–533.
9. Zeuthen, T., A. K. Meinild, D. D. Loo, E. M. Wright, and D. A. Klaerke. 2001. Isotonic transport by the Na+-glucose cotransporter SGLT1 from humans and rabbit. *J. Physiol.* 531:631–644.
10. Zeuthen, T., E. Zeuthen, and D. A. Klaerke. 2002. Mobility of ions, sugar, and water in the cytoplasm of *Xenopus* oocytes expressing Na(+)-coupled sugar transporters (SGLT1). *J. Physiol.* 542:71–87.
11. Loo, D. D., E. M. Wright, and T. Zeuthen. 2002. Water pumps. *J. Physiol.* 542:53–60.
12. Schultz, S. G. 2001. Epithelial water absorption: osmosis or cotransport? *Proc. Natl. Acad. Sci. USA.* 98:3628–3630.
13. Spring, K. R. 1999. Epithelial fluid transport: a century of investigation. *News Physiol. Sci.* 14:92–98.
14. Reuss, L., and B. H. Hirst. 2002. Water transport controversies: an overview. *J. Physiol.* 542:1–2.
15. Reuss, L. 1996. Active' water transport? *J. Physiol.* 497:1.
16. Bourgeois, F., M. J. Coady, and J. Y. Lapointe. 2005. Determination of transport stoichiometry for two cation-coupled myo-inositol cotransporters: SMIT2 and HMIT. *J. Physiol.* 563:333–343.
17. Hediger, M. A., E. Turk, and E. M. Wright. 1989. Homology of the human intestinal Na+/glucose and *Escherichia coli* Na+/proline cotransporters. *Proc. Natl. Acad. Sci. USA.* 86:5748–5752.
18. Bissonnette, P., J. Noel, M. J. Coady, and J. Y. Lapointe. 1999. Functional expression of tagged human Na+-glucose cotransporter in *Xenopus laevis* oocytes. *J. Physiol.* 520:359–371.
19. Coady, M. J., F. Jalal, P. Bissonnette, M. Cartier, B. Wallendorff, G. Lemay, and J. Lapointe. 2000. Functional studies of a chimeric protein containing portions of the Na(+)/glucose and Na(+)/myo-inositol cotransporters. *Biochim. Biophys. Acta.* 1466:139–150.
20. Steiner, R. A., M. Oehme, D. Ammann, and W. Simon. 1979. Neutral carrier sodium ion-selective microelectrode for intracellular studies. *Anal. Chem.* 51:351–353.
21. Jaisser, F., P. Jaunin, K. Geering, B. C. Rossier, and J. D. Horisberger. 1994. Modulation of the Na,K-pump function by beta subunit isoforms. *J. Gen. Physiol.* 103:605–623.
22. Meinild, A., D. A. Klaerke, D. D. Loo, E. M. Wright, and T. Zeuthen. 1998. The human Na+-glucose cotransporter is a molecular water pump. *J. Physiol.* 508:15–21.
23. Loo, D. D., B. A. Hirayama, A. K. Meinild, G. Chandy, T. Zeuthen, and E. M. Wright. 1999. Passive water and ion transport by cotransporters. *J. Physiol.* 518:195–202.
24. Zeuthen, T., and D. A. Klaerke. 1999. Transport of water and glycerol in aquaporin 3 is gated by H(+). *J. Biol. Chem.* 274:21631–21636.
25. Lide, D. R. 2004. Handbook of Chemistry and Physics.
26. Eskandari, S., E. M. Wright, and D. D. Loo. 2005. Kinetics of the reverse mode of the Na+/glucose cotransporter. *J. Membr. Biol.* 204: 23–32.
27. Sauer, G. A., G. Nagel, H. Koepsell, E. Bamberg, and K. Hartung. 2000. Voltage and substrate dependence of the inverse transport mode of the rabbit Na(+)/glucose cotransporter (SGLT1). *FEBS Lett.* 469: 98–100.
28. Meinild, A. K., D. D. Loo, A. M. Pajor, T. Zeuthen, and E. M. Wright. 2000. Water transport by the renal Na(+)-dicarboxylate cotransporter. *Am. J. Physiol. Renal Physiol.* 278:F777–F783.
29. Valentine, M. T., Z. E. Perlman, T. J. Mitchison, and D. A. Weitz. 2005. Mechanical properties of *Xenopus* egg cytoplasmic extracts. *Biophys. J.* 88:680–689.